Natural Hazards
https://doi.org/10.1007/s11069-020-04096-4

ORIGINAL PAPER

Assessing storm surge impacts on coastal inundation due to climate change: case studies of Baltimore and Dorchester County in Maryland

Ming Li[1] · **Fan Zhang**[1] · **Samuel Barnes**[2] · **Xiaohong Wang**[2]

Received: 9 January 2019 / Accepted: 30 May 2020

Abstract
Hurricane Isabel (2003) generated record flooding around Chesapeake Bay and caused extensive damage in rural Eastern Shore of Maryland and metropolitan cities like Baltimore. Regional atmosphere–ocean models are used to investigate the storm surge and coastal inundation that might be produced by a similar storm under the warmer ocean temperature and higher sea level projected for the future climate. Warming causes the storm to intensify, with the minimum sea level pressure decreasing from 955 mb during Isabel to ~ 950 mb in 2050 and ~ 940 mb in 2100. The stronger storm and higher mean sea level amplify the peak water level by ~ 0.5 m in 2050 and ~ 1.2 m in 2100. The total inundated area over Chesapeake Bay expands by 26% in 2050 and 47–62% in 2100. Over the rural Dorchester County, the inundated area shows moderate expansion in the future climate but the average inundation depth is 30% higher in 2050 and 50–70% higher in 2100. The number of houses flooded increases from 1420 during Hurricane Isabel to 1850/2190 in 2100 under the climate change scenario representative concentration pathway (RCP) 4.5/8.5. The inundated area in Baltimore is 2.2 km^2 during Hurricane Isabel, expands to 5.1 km^2 in 2050, and reaches 8.1/9.1 km^2 in 2100 under RCP 4.5/8.5. The estimated flood damage to Baltimore increases from $29 million in 2003 to $98/100 million in 2050 and $150/162 million in 2100 under the median projection of RCP 4.5/8.5. These estimates are subjected to uncertainty due to different climate change scenarios and different climate model projections.

Keywords Coastal inundation · Climate change · Sea level rise · Storm surge · Economic loss · Impact assessment

✉ Ming Li
mingli@umces.edu

[1] Horn Point Lab, University of Maryland Center for Environmental Science, Cambridge, MD 21613, USA

[2] Department of Mathematics and Computer Science, Salisbury University, 1101 Camden Avenue, Salisbury, MD 21801, USA

Published online: 06 June 2020

1 Introduction

As demonstrated during recent catastrophic events such as Hurricane Sandy (2012), Hurricane Harvey (2017), and Hurricane Irma (2017), coastal communities, properties, and natural resources are at great risk to coastal inundation caused by storm surge. Since the nineteenth century, storm surge has cost millions of lives and hundreds of billions dollars in economic damage (El-Sabh 1990; USGCRP 2017). Climate change is expected to increase the rate of sea-level rise (IPCC 2013; Church et al. 2013) and cause significant increases in extreme weather (Emanuel 2008; Woolings et al. 2012; Knutson et al. 2013; Eichler et al. 2013), exacerbating the coastal inundation problem. There is thus an urgent need to assess the potential impacts of storms on coastal inundation in the future climate.

Sea level rise leads to higher extreme sea levels and more extensive coastal flooding (Hallegatte et al. 2013; Hinkel et al. 2014; Sweet and Park 2014; Moftakhari et al. 2015). Tide gauge records and satellite altimetry reveal that global-mean sea level (GSML) rose at a rate of 1.2 mm $\pm$ 0.2 yr^{-1} between 1900 and 1990 and at a much faster rate of 3.0 $\pm$ 0.7 mm yr^{-1} between 1993 and 2012 (Domingues et al. 2008; Church and White 2011; Hay et al. 2015; Dangendorf et al. 2017). Climate models predict that the rate of sea level rise will accelerate in the twenty-first century. According to IPCC AR5 (Fifth Assessment Report of the Intergovernmental Panel on Climate Change), GMSL is projected to rise 0.52–0.98 m by 2100 for the highest emission scenario considered—Representative Concentration Pathway (RCP) 8.5 (Church et al. 2013). Probabilistic sea level projections suggest a very likely (90% probability) GMSL rise of 0.5–1.2 m under RCP 8.5 (Kopp et al. 2014). If the rapid collapse of Antarctic ice sheet as projected in some climate models is taken into consideration, the median projected GMSL for 2100 will increase from 0.79 to 1.46 m under RCP 8.5 (Kopp et al. 2017).

Some parts of the ocean rise faster than others. For example, tide-gauge records in Chesapeake Bay show that sea levels increased by 3–4 mm per year over the twentieth century (Zervas 2001, 2009), twice that of the global average. Land subsidence associated with glacial isostatic adjustment is a dominant contributor to the high relative sea level rise (Engelhart et al. 2009; Miller et al. 2013). Ocean dynamics, arising from changing ocean circulation, may also contribute to higher sea levels in certain coastal regions. Sallenger et al. (2012) presented evidence that the US East Coast north of Cape Hatteras is a hot spot of sea level rise. The weakening of the Gulf Stream over the past decade may have contributed to the higher rates of sea level rise along the mid-Atlantic coast (Ezer and Corlett 2012; Ezer 2013; Ezer et al. 2013; Kopp 2013). The Atlantic Meridional Overturning Current (AMOC), of which the Gulf Stream is an essential component, is predicted to weaken during the twenty-first century (Yin et al 2009, 2010; Yin and Goddard 2013), further raising sea levels along the US East Coast. However, recent analysis showed that sea level declined north of Cape Hatteras between 2010 and 2015 and this decline was caused by an increase in atmospheric pressure combined with shifting wind patterns (Domingues et al. 2018). Pieuch et al. (2018) suggested that river discharge may be a driver of regional sea level variability along US East and Gulf coasts.

Will extreme weather events such as hurricanes become more frequent and more severe in a warming climate? Studies based on coarse-resolution general circulation models (GCMs) have generally agreed on a tendency toward decreasing frequency and increasing intensity of tropical cyclones as the climate warms (Bengtsson et al. 1996). On the other hand, a consensus of GCMs predicts increasing wind shear over the North Atlantic with warming (Vecchi and Soden 2007), which would tend to inhibit overall tropical

cyclone activity. Using an ensemble of GCMs and scenarios from phases 3 and 5 of the Coupled Model Intercomparison Project (CMIP3 and CMIP5), Knutson et al. (2013) conducted dynamic downscaling projections of the twenty-first century Atlantic hurricane activity. They found a significant reduction in the overall tropical storm frequency but a significant increase in the frequency of intense storms. Similar results were found in statistical-dynamic models (Emanuel 2006, 2008; Lin et al. 2012). However, Emanuel (2013) found that tropical cyclones over most oceans are projected to increase not only in intensity but also in frequency during the twenty-first century under RCP 8.5. Extratropical winter storms are also likely to change in the future climate. There is a remarkable consensus among climate models that the overall frequency of such storms will decline while the frequency of severe storms will increase (Woolings et al. 2012).

The combination of stronger storms and sea level rise will likely result in higher water levels and more extensive inundation in the future climate. However, assessing the climate change impacts on coastal inundation faces many challenges. Chief among them are the large uncertainty in sea level rise projections in the second half of twenty-first century (Kopp et al. 2017), the inherent difficulty of global climate models in predicting future storms, long-term geomorphological changes in coastal regions (Bilskie et al. 2016), and coastline management decisions under the threat of climate change and sea level rise (Holleman and Stacey 2014; Lee et al. 2017; Zhang and Li 2019). Moreover, engineering projects such as navigation channel dredging have led to significant increases in tidal range and storm surge height in many estuaries, including the Cape Fear River estuary, North Carolina (Familkhalili and Talke 2016) and the Hudson River estuary (Ralston et al. 2019). Interestingly, however, the mean water level in the upper part of the Hudson River decreased as a result of channel deepening such that the overall flooding risk was reduced.

Several methods have been proposed to examine the coastal inundation risk under a changing climate: dynamic climate downscaling approach, statistical deterministic approach, and perturbed historical baseline approach (Mcinnes et al. 2003; Bilskie et al. 2016). In the dynamic downscaling approach, high-resolution regional atmosphere models capable of simulating hurricanes and tropical storms are nested within the coarse-resolution GCMs under the future climate condition (Lowe and Gregory 2005; Knutson and Tuleya 2004; Woth et al. 2006; Mallard et al. 2013a, b; Knutson et al. 2013). This is the most direct approach for assessing the climatic impacts on storms but is computationally prohibitive and inherits biases in the GCMs. In the statistical deterministic model, synthetic storms are generated from a statistical deterministic hurricane model (Emanuel et al. 2006) under large-scale atmospheric and oceanic environments as projected by GCMs (Mousavi et al. 2011; Hagen and Bacopoulos 2012; Lin et al. 2012, 2016). Using these synthetic storms to drive a hydrodynamic model, Lin et al. (2012) showed that the combined effects of storm climatology change and 1 m sea level rise may cause the present New York City 100-year surge flooding to occur every 3–20 years by the end of twenty-first century. In the perturbed historical approach, the hydrodynamic model is forced with historical extreme sea levels to obtain a baseline, and changes to the mean seal level and hurricane intensity are included in the model simulations (Yang et al. 2014; Orton et al. 2015, 2018). A few studies use a hybrid of these approaches. For example, Mousavi et al. (2011) investigated three historical storms and used an empirical deterministic model to account for the changes in the storm intensity due to warming ocean.

Previous studies have suggested that the cumulative effects of sea level rise, tides and storm surges on coastal inundations are not simple linear additions. Smith et al. (2010) found that sea level rise can greatly amplify surge heights in shallow wetland areas of southeast Louisiana. Surge generation and propagation over shallow areas are nonlinear

processes and sensitive to changes in the water depth. There are also strong interactions between storm surges and tides (Horsburgh and Wilson 2007). Mikhailva (2011) examined sea level observations in the Elbe River, Germany, and found that mean sea level, tidal range, and storm surges all increased during the second half of the twentieth century. When changes in storm climate are considered, Lin et al. (2016) found that Hurricane Sandy's flooding frequency at New York City significantly increases over twenty-first century compared to the scenario with sea level rise alone. Large-scale climate variabilities such as the North Atlantic Oscillation and geomorphic changes due to dredging or shoreline hardening may have also contributed to higher sea level extremes in recent decades (Talke et al. 2014; Marcos et al. 2015; Familkhalili and Talke 2016; Ralston et al. 2019).

Besides the physics of sea level rise, storm surge, and extreme sea levels, a number of studies have investigated the socioeconomic impacts of coastal flooding (e.g., Nicholls 2004; Hinkel et al. 2013; McNamara et al. 2015; Kulp and Strauss 2017; McAlphine and Porter 2018). For example, Hinkel et al. (2014) estimated that 0.2–4.6% of global population will be flooded annually in 2100 under 0.25–1.23 m GMSL rise, with expected annual loss of 0.3–9.3% of global domestic product. For the USA, Hauer et al. (2016) projected that a 2100 sea level rise of 0.9 m will put 4.2 million people at the risk of coastal inundation. Neumann et al. (2015) examined the joint effects of storm surge and sea level rise in economic damage. Dinan (2017) suggested that the combined forces of climate change and coastal development will cause hurricane damage to increase faster than the US economy which is expected to grow in the twenty-first century. Other studies have analyzed how coastal mitigation and adaptation may alleviate the socioeconomic impacts of coastal inundation (e.g., Neumann et al. 2011; Hallegatte et al. 2013). For example, Diaz (2016) used an optimization model to determine the optimal strategy for adaptation. McNamara et al. (2015) developed a stochastic dynamic model coupling coastal property markets and shoreline evolution and found that the policy-induced inflation of property value grows with increased erosion from sea level rise or increased storminess.

The coastal plains surrounding Chesapeake Bay feature many low-lying areas with low topographic relief (Wu et al. 2009) and are thus a good site for studying coastal inundation in a changing climate. Recurrent flooding at high tides is already a major problem (Mitchell et al. 2012) and will likely become more frequent in the future as sea level rises (Spanger-Siegfried et al. 2014). Chesapeake Bay is also susceptible to flooding by storm surges: About two dozens of hurricanes and tropical storms have moved past the Chesapeake Bay region over the past 20 years. In particular, Category 2 Hurricane Isabel made landfall over the Outer Banks of North Carolina on 18 September 2003 and moved northward on the west side of Chesapeake Bay, creating widespread flooding in Norfolk, Washington, D.C., Annapolis, Baltimore and rural Eastern Shore of Maryland and Virginia (Li et al. 2006, 2007; Shen et al. 2006; Zhong et al. 2010), as shown in Fig. 1. This flooding event is considered to be a 100-year flooding event for planning purposes by cities and towns around Chesapeake Bay. A major open question is how much flooding such a storm may generate in 2050 or 2100 when the mean sea level and ocean temperature are higher. To address this, we use regional atmosphere–ocean models to simulate Hurricane Isabel (2003) and Isabel-like storms in the future climate as projected by the global climate models. Our approach goes beyond previous studies on storm surge because a regional atmosphere model is used to directly simulate the effects of ocean warming on hurricanes. Unlike the parametric surface wind model/planetary boundary wind model (Scheffner and Fitzpatrick 1997; Peng et al. 2004) and statistical-deterministic models (Lin et al. 2012, 2016), the regional atmosphere model can simulate the full hurricane dynamics including mesoscale wind structures and wind speed asymmetry. An accurate wind field is critical for an accurate prediction of storm surge along complex coastlines such

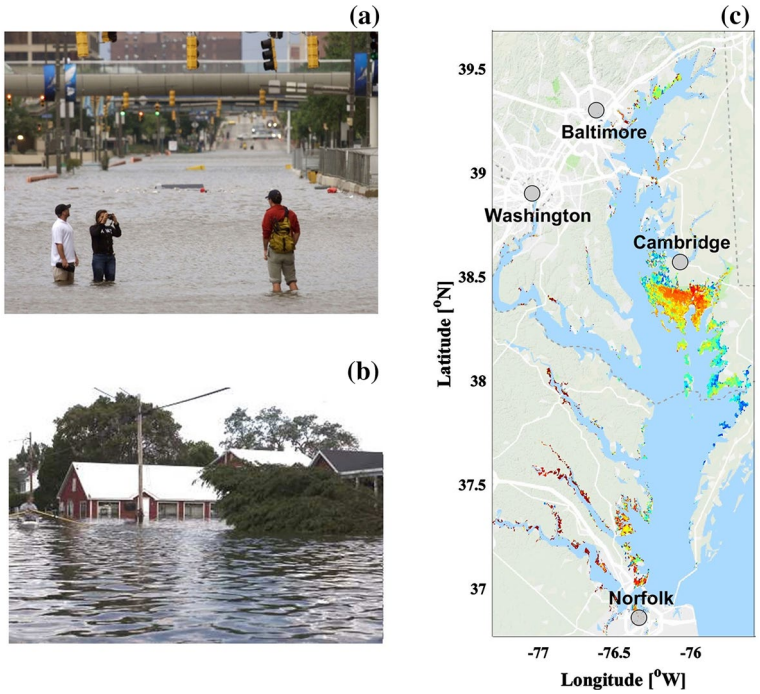

Fig. 1 Photographs of flooding scenes in **a** Baltimore and **b** Dorchester County, MD, during Hurricane Isabel (2003). **c** Model-predicted inundated areas around Chesapeake Bay region during Isabel

as estuaries and bays (Chen et al. 2013; Kerr et al. 2013). Coastal inundation maps obtained from the regional atmosphere–ocean models will provide a more realistic depiction of coastal flooding over land during a storm than those obtained from a storm surge model forced by the parametric winds of a hurricane vortex.

We will investigate first the storm surge and coastal inundation over the entire estuary and then provide detailed assessments on flooding and economic damage at two representative sites. The City of Baltimore is chosen as a representative urban site, and the Dorchester County on the Eastern Shore of Maryland is chosen as a representative rural area. By comparing the responses of an urban and a rural site to the same storms, we can gain a better understanding of their risks. Our goal is not to produce a probabilistic prediction for the storm surge and flooding in the mid- and late twenty-first century but rather to illustrate how ocean warming and sea level rise affect the peak water level and coastal inundation in a coastal region. Although similar studies were conducted on other coastal waters, storm surge response to hurricanes is highly dependent on bathymetry and coastline geometry. The semi-enclosed nature of an estuary like Chesapeake Bay can trap and amplify storm flooding, making it particularly vulnerable to coastal inundation.

2 Methods

To assess potential impacts of climate change on storm surge and coastal inundation, we use regional atmosphere and ocean models. The regional atmosphere model, based on Weather Research and Forecasting (WRF) model, simulates how ocean warming affects storm intensity. The regional ocean model, based on the Finite Volume Coastal Ocean Model (FVCOM), simulates how sea level rise affects storm surge and overland inundation. The model-predicted peak surge levels are projected onto low-lying land areas to assess their impacts on coastal communities.

2.1 Regional atmospheric model

WRF is a non-hydrostatic, mesoscale atmospheric model (Skamarock et al. 2008) and has been widely used for hurricane simulations (e.g., Davis et al. 2008; Nolan et al. 2009a, b; Seroka et al. 2016). We configured triple-nested model domains for WRF (Fig. 2a). The outermost domain covers the western Atlantic at a coarse resolution of 12 km. The middle domain covers the south and middle Atlantic regions at a resolution of 4 km. The innermost domain uses a fine resolution of 1.33 km to resolve the Chesapeake Bay region. There are 40 vertical sigma levels. At the lateral boundaries of its outermost domain, WRF is forced by 6-hourly final (FNL) operational global analysis data at 1° spatial resolution (https://rda.ucar.edu/datasets/ds083.2/). At the ocean surface, WRF is forced by outputs from daily real-time global SST sea surface temperature (SST) with 0.5° resolution (hereafter RTG-SST, https://polar.ncep.noaa.gov/sst/rtg_low_res/). FNL is also used to initialize WRF at approximately 48 h prior to the hurricane's landfall. Zhang et al. (2017) used this WRF model to simulate Hurricane Arthur (2014) and obtained good agreements between the predicted and observed storm track, storm intensity and forward propagation speed.

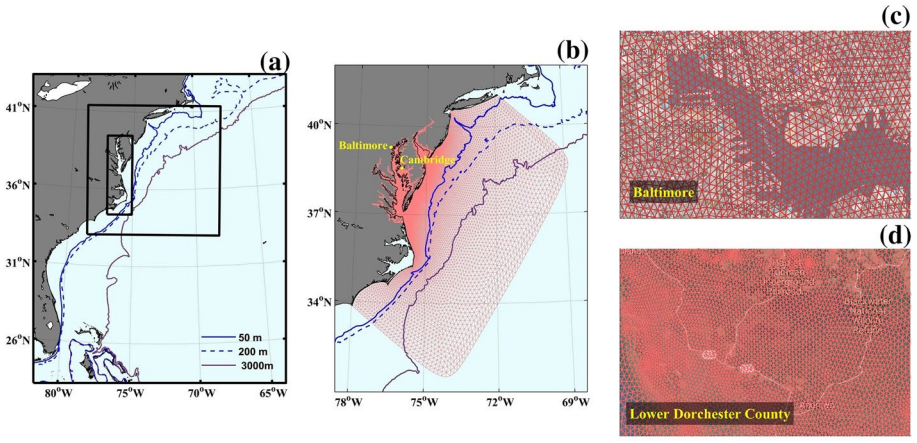

Fig. 2 **a** Triple-nested WRF model domains (denoted by the thick black boxes) with resolutions of 12, 4, and 1.33 km. **b** FVCOM model grids (red) in which the two yellow dots mark the locations of tidal gauge stations in Cambridge and Baltimore, MD. Zoomed-in view of fine-resolution FVCOM grids for **c** the City of Baltimore and **d** Dorchester County, MD

2.2 Regional ocean model

The unstructured-grid FVCOM was used to simulate storm surge and overland inundation (Chen et al. 2003, 2006). The model domain covers Chesapeake Bay and the eastern US continental shelf (Fig. 2b). The horizontal resolution ranges from ~ 1 km in the inner shelf to ~ 10 km near the open boundaries. The model resolves Chesapeake Bay and its surrounding lands (up to 5 m height above the current mean sea level) at a resolution of 0.2–1.0 km. Finer resolutions are placed over the City of Baltimore (5–10 m) (Fig. 2c) and the rural eastern shore of Maryland including Dorchester County (100–200 m) (Fig. 2d), two focus areas in this study. About 25% of the Chesapeake Bay shoreline is hardened, but these structures mostly use shoreline stabilization techniques such as riprap and bulkheading and do not provide much protection against flooding (Patrick et al. 2014; Palinkas et al. 2017). These small engineered structures are not resolved in the FVCOM model. Neither are small-scale offshore engineered structures such as bridge piers, breakwaters, and groynes.

The model is run in three-dimensional barotropic mode in which temperature and salinity are kept constant. In the vertical direction, five sigma layers are used. At the offshore open boundary, the sea level is prescribed using ten tidal constituents according to the Oregon State University global tidal model TOPEX/POSEIDON 7.1 (Egbert and Erofeeva 2002). Hourly outputs of surface wind and air pressure fields from WRF are used to drive FVCOM. A quadratic stress is exerted at the bed, with the bottom roughness height set to be 2 mm in Chesapeake Bay and 2 cm on the adjacent shelf (Lee et al. 2017). As a simplification, the roughness heights are assumed to be the same between the sea beds and the surrounding lands. We also ran the model with a uniform roughness height and only found minor differences in the storm surge prediction. FVCOM simulation started at about 1 week before a hurricane's landfall to give sufficient time for the model to spin up.

To simulate overland inundation, coastal lands up to 5 m above the mean sea level are included in the model domain. High-resolution (10-m horizontal resolution) digital elevation data in land areas surrounding Chesapeake Bay are obtained from US Geological Survey National Elevation Dataset (Gesch 2009) while the elevation data (at a resolution of 1/3 arc-second) for areas along the open coast are obtained from NOAA's Coastal Relief Model data (e.g., Grothe et al. 2010). Bathymetry data are acquired from the NOAA 1 arc second resolution Bathymetric Digital Elevation Model in estuaries, the 3 arc second Coastal Relief Model on the continental shelf, and the 1 arc-minute ETOPO1 Global Relief Model in the deep ocean (Amante and Eakins 2009). Raw elevation and bathymetry data referenced to different vertical datum are converted to the same vertical coordinate system (NAVD88) using the V-Datum program (Yang et al. 2008; Lee et al. 2017).

Wetting and drying of grid cells is implemented to simulate overland inundation due to storm surge and sea level rise. FVCOM uses a point treatment technique in which numerical grids consist of wet and dry points with a boundary defined as an interface line between the water and land, respectively (Chen et al. 2011). A grid is treated as a wet point when the water depth exceeds h_c(set to be 5 cm in our model), otherwise it is considered a dry point at which velocities are set to zero.

2.3 Design of numerical experiments

To project the impact of climate change on coastal inundation in 2050 and 2100, we make use of the Intergovernmental Panel on Climate Change fifth assessment report (IPCC AR5). The IPCC AR5 projections are based on a set of greenhouse gas concentration scenarios called Representative Concentration Pathways that reflect the updated greenhouse gas emission reduction possibilities and climate change stabilization goals (Moss et al. 2010; van Vuuren et al. 2011). We selected RCP 4.5 and 8.5, representative of medium (delayed action) and high (growing) emission scenarios, respectively. The Coupled Model Intercomparison Project Phase 5 (CMIP5) used in the IPCC AR5 contains 15 general circulation models (GCMs). We extracted sea surface temperature (SST) in the tropical Atlantic Ocean from these GCMs and calculated the SST difference between the future climate and the historical reference period 1986–2005 (Villarini and Vecchi 2012). Then, the GCMs with minimum, median, and maximum SST changes were selected for the downscaling simulations. The median projection is for the SST to increase by 1.13 and 1.71 °C at 2050 and by 1.48 and 2.94 °C at 2100, with the lower values from RCP 4.5 and the higher values from RCP 8.5 (Table 1). The inter-model spread in SST is larger in 2100 than in 2050, reflecting larger uncertainty in the projection for the end of twenty-first century.

The GCMs are also used to project the future sea level rise, but local effects such as land subsidence and ocean dynamics in the northwest Atlantic Ocean are included. Church et al. (2013) analyzed individual contributions to sea level rise and estimated the median values and likely ranges for projections of GMSL in the twenty-first century relative to 1986–2005. The median, lower, and upper range of GMSL will be used to obtain the median, lower, and upper range for the relative sea level rise in Chesapeake Bay. The regional land subsidence due to glacial isostatic adjustment was estimated following Miller et al. (2013). The regional sea level rise due to changing ocean dynamics was estimated

Table 1 Projected increases in sea surface temperature (SST) in the Atlantic ocean and relative sea level rise in Chesapeake Bay. The 'median,' 'minimum,' and 'maximum' scenarios are based on the median value and likely lower and upper bounds of projected global mean sea level rises in the IPCC AR5 report

	RCP 4.5			RCP 8.5		
	Median	Minimum	Maximum	Median	Minimum	Maximum
2050						
SST increase in Tropical North Atlantic (°C)	1.13	0.83	2.11	1.71	1.20	2.64
Global mean sea level rise	0.26	0.19	0.33	0.30	0.22	0.38
Regional ocean dynamics	0.09	0.07	0.10	0.09	0.07	0.1
Regional land subsidence	0.075	0.065	0.085	0.075	0.065	0.085
Relative sea level rise (m)	0.43	0.33	0.52	0.47	0.36	0.57
2100						
SST increase in Tropical North Atlantic (°C)	1.48	0.98	2.54	2.94	2.30	4.24
Global mean sea level rise	0.53	0.36	0.71	0.74	0.52	0.98
Regional ocean dynamics	0.17	0.13	0.19	0.17	0.13	0.19
Regional land subsidence	0.15	0.13	0.17	0.15	0.13	0.17
Relative sea level rise (m)	0.85	0.62	1.07	1.06	0.78	1.34

according to Yin et al. (2009). Adding the three components together yielded the relative sea level rise in 2050 and 2100, as shown in Table 1. Our median estimate is nearly the same as Kopp et al. (2014)'s central estimate for the relative sea level rise in Chesapeake Bay while the lower (min) and upper (max) bounds correspond to the two endpoints of their likely range (67% probability). In a recent study, Kopp et al. (2017) considered DP16 (DeConto and Pollard 2016) scenarios in which the rate of the sea level rise would be much higher due to possible rapid loss of the polar ice sheets such as the deterioration of Antarctic ice shelves. DP16 scenarios were not considered in this study. More detailed information on the configuration of numerical experiments for climate change scenarios can be found in Zhang and Li (2019).

We conducted a total of 13 numerical experiments. The control run was the hindcast simulation of Hurricane Isabel (2003) which served as the baseline to assess the climate change impacts. For Isabel, WRF was forced by the FNL operational global analysis data at the lateral boundary and by daily RTG-SST at the ocean surface. For Isabel-like storms in 2050 and 2100, WRF-FVCOM incorporated the effects of ocean warming and relative sea level rise under the median, lower, and upper range projections from RCP 4.5 and 8.5. Since the GCMs do not have adequate resolutions to predict hurricanes in the future climate, they were not used to force WRF. Instead WRF was forced by FNL at the lateral boundary. At the ocean surface, however, the GCM's projected increase in the SST was added to RTG-SST to set the ocean surface boundary condition for WRF. Following Hill and Lackmann (2011) and Mallard et al. (2013a), the GCM-projected changes in the atmosphere temperature between the historical period and future climate were averaged horizontally over the tropical Atlantic Ocean and then added to the FNL outputs to set the initial and lateral boundary conditions for WRF (see also Zhang and Li 2019). This approach provided a cost-effective alternative to running high-resolution regional climate models (Knutson et al. 2013) and captures changes in the atmospheric thermal conditions (temperature and moisture) associated with warmer SST. To account for the relative sea rise in FVCOM, the projected increase in the mean sea level was superimposed onto the astronomical tides along the open boundary of FVCOM. This is a simplified representation of the sea level rise, which changes coastlines gradually. To model geomorphic response to sea level rise, one would need to develop a coupled hydrodynamic-wave-sediment transport model to simulate shoreline erosion and deposition processes, but it is computationally prohibitive to run such a model for 50 and 100 years. One would also need to consider the role of coastal wetlands in shaping coastline changes under changing climate.

2.4 Inundation impact analysis

Google Map and Google Earth are used to visualize inundations over the land areas surrounding Chesapeake Bay, including City of Baltimore and Dorchester County in Maryland. Water level data from FVCOM were imported and overlaid on Google Map and Google Earth. Inundation depths were obtained by subtracting the digital elevation data from the water level in each grid cell. The result was a wet/dry profile of inundation. Google Earth allows users to add and view 3D buildings, thus enabling 3D views of inundations over buildings and structures.

A majority of the data used for the inundation impact analysis were collected from US Census Bureau (https://www.census.gov/data.html) and housing websites such as Trulia (https://www.trulia.com) and Zillow (https://www.zillow.com). Dorchester County was chosen as a representative rural site. It is the largest county in Maryland and has a total

area of 983 square miles (2550 km^2). According to the census in 2010, the county had a population of 32,618 and a population density of 55 people per square mile (www.census.gov/quickfacts/dorchestercountymaryland, www.dorchestercountymd.com/). There were 14,681 housing units at an average density of 26 per square mile, with the average home value of $188,000. The average household size was 2.36, and the average family size was 2.86. Model-predicted inundated areas for Dorchester County were combined with the census and housing data to estimate numbers of houses and people affected by flooding. The total depth-damage function for residential houses, which includes structure and content costs, was used to estimate the flood damage, following the approach adopted by FEMA (Federal Emergency Management Agency) HAZUS-MH (Hazards US for Multi-Hazard Earthquakes, Hurricanes and Floods) program (Scawthorn et al. 2006a, b; Ding et al. 2008; HAZUS 2014).

The City of Baltimore was chosen as a representative urban site. It is the largest city in Maryland, with a population of 2.81 million in the Baltimore metropolitan area. The city has a total area of 92.1 square miles (239 km^2). Baltimore is densely populated, with approximately 7671 people per square mile (https://www.census.gov/quickfacts/fact/table/baltimorecitymaryland). Founded in 1729, Baltimore harbor is the second-largest seaport in the mid-Atlantic where millions of shipments are made every single year. Baltimore has about 50,800 firms where many of these firms and businesses are located on or near the waterfront. As a large city, 93% of the homes in Baltimore are multi-unit buildings such as apartments, but a majority of the properties in downtown Baltimore are commercial buildings. To estimate the flood damage to Baltimore, we used the total depth-damage function appropriate for commercial buildings, including structure and content costs (Scawthorn et al. 2006a, b; Smith 1994; Huizinga et al. 2017). We did not index for future price increases/decreases in real estate. The purpose of this inundation impact analysis is not to obtain a precise estimate for the economic loss caused by coastal inundation but rather to examine relative changes in the storm surge damage due to climate change.

3 Results

A hindcast simulation of Hurricane Isabel (2003) was conducted first and then compared against simulations of a similar storm under the higher SST and sea level projected by the climate models. The bay-wide response is presented first, followed by detailed analyses on Dorchester County and City of Baltimore.

3.1 Bay-wide response

Hurricane Isabel made landfall at the Outer Bank of North Carolina on 18 September 2003 and travelled northwestward along a nearly straight line that began 2 days before landfall and lasted until its eventual dissipation over the Great Lakes. WRF accurately predicted Isabel's track and forward propagation speed (Fig. 3a). The root-mean-square error (RMSE) between the predicted and observed tracks is 29.3 km. The observed minimum sea level pressure (MSLP) reached a low of 955 mb on late 17 September, but rebounded to 1000 mb on 19 September. WRF captured the observed temporal evolution of storm intensity (Fig. 3b). Isabel attained a maximum sustained wind (MSW) of 45 m s^{-1} at 10 m above the sea surface. This was well simulated by WRF, although WRF slightly overestimated MSW post-landfall (Fig. 3c). The RMSE for MSLP and

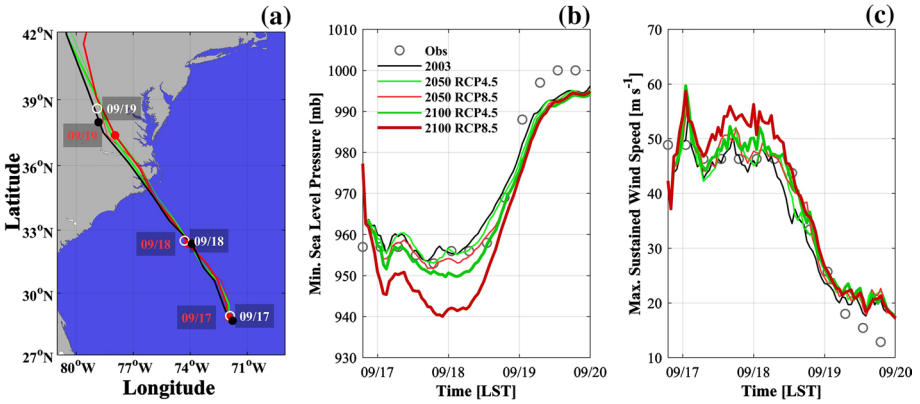

Fig. 3 **a** Hurricane tracks, time series of **b** minimum sea level pressure (MSLP) and **c** maximum sustained wind speed (MSW) for Hurricane Isabel in 2003 (black) and Isabel-like storms in 2050 (thin lines) and 2100 (thicker lines). Open circles mark the observed MSLP and MSW during Hurricane Isabel. Green/red lines represent the median climate projections in RCP4.5/8.5

MSW is 6.9 mb and 4.3 m s^{-1}, respectively, while the correlation coefficients are 0.94 and 0.96. The RMSE normalized by variances is 0.020/0.024 for MSLP/ MSW.

When exposed to warmer SST in the future climate, the storm intensifies. MSLP decreases to a minimum of 952 mb in 2050 and 940–950 mb in 2100 (Fig. 3b). The MSLP difference between the median RCP 4.5 and 8.5 projections is about 2 mb in 2050 but reaches 10 mb in 2100. MSW also becomes much stronger in the future climate: increasing from a peak speed of 45 m s^{-1} during Isabel to ~ 50 m s^{-1} in 2050 and ~ 55 m s^{-1} in 2100 (Fig. 3c). Since the same large-scale atmospheric flow fields (FNL) were used to force WRF at the lateral boundary, the storm in the future climate follows essentially the same track as Hurricane Isabel (Fig. 3a).

The stronger storm results in higher storm surge. Together with sea level rise, high water levels are generated in Chesapeake Bay. Two tidal gauge stations were selected for comparing the sea level time series (their locations marked in Fig. 2b). The Cambridge tidal gauge is located in the mid-Bay, next to Dorchester County. The Baltimore tidal gauge is located next to the Inner Harbor of downtown Baltimore. The observed peak surge height during Hurricane Isabel was 1.6 m in Cambridge and 2.3 m in Baltimore. FVCOM accurately predicted the storm surge: The RMSE is 0.15 m, and the correlation coefficient is 0.97 (Fig. 4a, c). The normalized RMSE is 0.035 in Cambridge and 0.040 in Baltimore. In 2050, the surge height is ~ 2.1 m in Cambridge and ~ 2.7 m in Baltimore. The difference in the median projection of the peak surge height between RCP 4.5 and RCP 8.5 is small, but the difference in the surge height between the lower and upper range of RCP 4.5/8.5 is 0.28/0.27 m in Cambridge and 0.27/0.36 m in Baltimore. Because the storm's forward propagation speed in 2050 is slightly slower than that during Isabel (Fig. 3a), the storm surge reaches its peak water level 1–2 h later at Cambridge and Baltimore. More dramatic differences in the peak water level are found in the model projections for 2100 (Fig. 4b, d). The peak water level from the median climate change projections increases to 2.5/2.7 m (RCP 4.5/8.5) in Cambridge and 3.2/3.4 m (RCP 4.5/8.5) in Baltimore. The spread among the model projections is considerably larger in 2100, with a surge height difference of 0.6 m in Cambridge and 0.7 m in Baltimore under RCP 8.5.

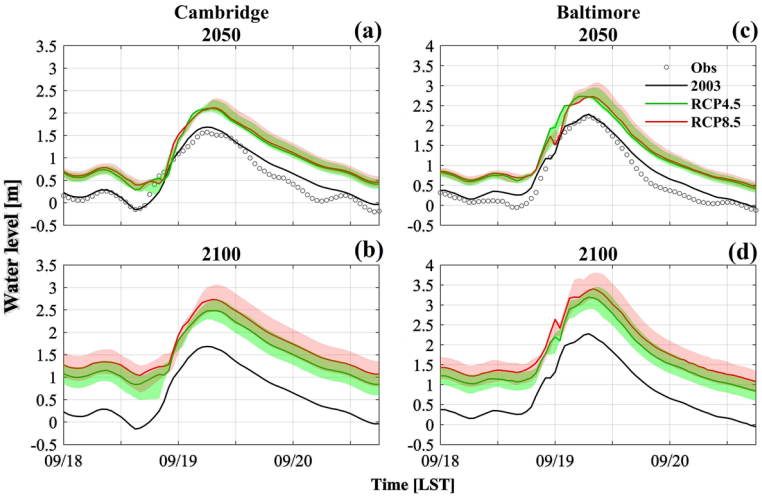

Fig. 4 Storm surge generated at Cambridge, MD (left, **a**, **b**), and Baltimore, MD (right, c and d), by Hurricane Isabel (2003) and Isabel-like storms in 2050 (**a**, **c**) and 2100 (**b**, **d**). The open circles represent the observed surge during Isabel, and the black line represents the model prediction. The green/red lines represent the water level projection under the median condition in RCP 4.5/8.5 while the shades represent the spreads among the GCM models

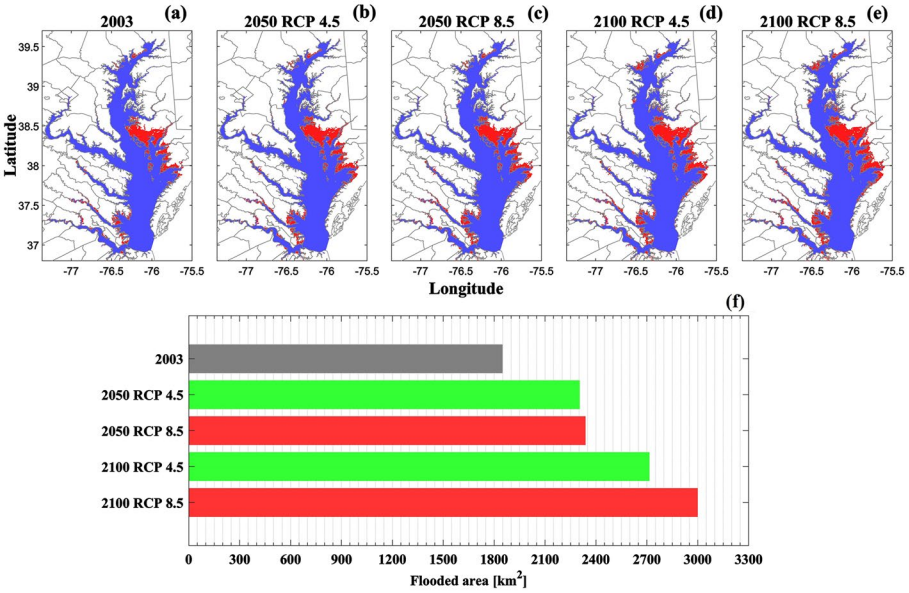

Fig. 5 **a**–**e** Flooded areas (red) around Chesapeake Bay during Hurricane Isabel (**a**) and Isabel-like storms in 2050 (**b**, **c**) and 2100 (**d**, **e**) (the present-day water surface in Chesapeake bay is shown as blue). **f** Total flooded area during Hurricane Isabel and under different climate change scenarios

The higher water levels lead to more extensive inundation around Chesapeake Bay (Fig. 5). During Hurricane Isabel, a large area on the eastern shore of Maryland was flooded, as well as near-shore regions in the lower Chesapeake Bay and isolated spots on the western shore of the northern Chesapeake Bay (Fig. 5a). These are low-lying land areas vulnerable to coastal inundation. In 2050, the flooded areas expand from these regions (Fig. 5b, c). By 2100, flooding appears at many locations along the coastlines of Chesapeake Bay and its tributaries, in addition to the eastern shore (Fig. 5d, e). Figure 5f compares the size of the inundated areas between Hurricane Isabel and Isabel-like storms in the future climate. Isabel flooded 1850 km^2. A similar storm in 2050 floods 2305/2339 km^2 under the median projections of RCP 4.5/8.5. By 2100, an Isabel-like storm floods 2,715 km^2 under RCP 4.5 median scenario and 3000 km^2 under RCP 8.5 median scenario, representing 47–62% increase in the flooded area over that during Hurricane Isabel. The total flooded area in 2100 varies from 2674 to 3359 km^2 between the upper and lower projections of RCP 8.5, representing ±11% uncertainty around the median projection. In comparison, a ± 5 cm error in the vertical datum would only result in ±3% differences in the inundation area. Most of the additional flooded areas are on the rural eastern shore of Maryland and Virginia where agricultural fields and wetlands dominate the landscape. The waterfront areas in cities like Norfolk, Washington, D.C., Annapolis, and Baltimore will be also be flooded, consisting mostly of commercial properties and apartment buildings.

Additional calculations were done to separate the contributions of sea level rise and storm surge to the total inundation area in the future climate. In 2050, sea level rise alone caused 599/688 km^2 to be flooded under the median projection of RCP 4.5/8.5. The additional inundated areas caused by storm surge were 1706/1653 km^2, smaller than the area flooded by Isabel (2003). A similar result was found for 2100: sea level rise flooded 1184/1484 km^2 under the median RCP 4.5/8.5 projection and the storm surge flooded additional 1531/1586 km^2. The land topography surrounding Chesapeake Bay rises more steeply away from the coastline, such that additional land areas flooded by storm surge would be smaller for the same surge height in the future climate.

3.2 Rural Dorchester County

Due to its shape, Dorchester County is known as heart of the Chesapeake (Fig. 6). Cambridge, the county seat with the highest population density, is located on the shore of the Choptank River in northern Dorchester County. The leaf-like parcel of land extends from Cambridge towards the main stem of Chesapeake Bay and is sandwiched between the Choptank River and the Little Choptank River. Along the coastline further south lies Taylor Island and Hooper Island. The Blackwater National Wildlife Refuge occupies the central part of southern Dorchester County. The refuge and the lands further south are low-lying areas vulnerable to coastal inundation. There are only a handful of major roads linking rural communities and fishing villages in Dorchester County, making emergency evacuation challenging.

When Hurricane Isabel hit in September 2003, the southern Dorchester County and parts of the leaf-like area in the northwest corner were flooded: the water depth was less than 0.5 m in the northwest but reached about 1.5 m over the Blackwater area (Fig. 7a). According to the median projections of RCP 4.5 and 8.5, the flooded areas show a modest expansion by 2050, because land elevation rises steeply further north (Fig. 7b, c). However, the inundation depth is significant higher. By 2100, the flooded areas expand towards higher grounds in the northeast direction (Fig. 7d, e). In addition, flooding appears along

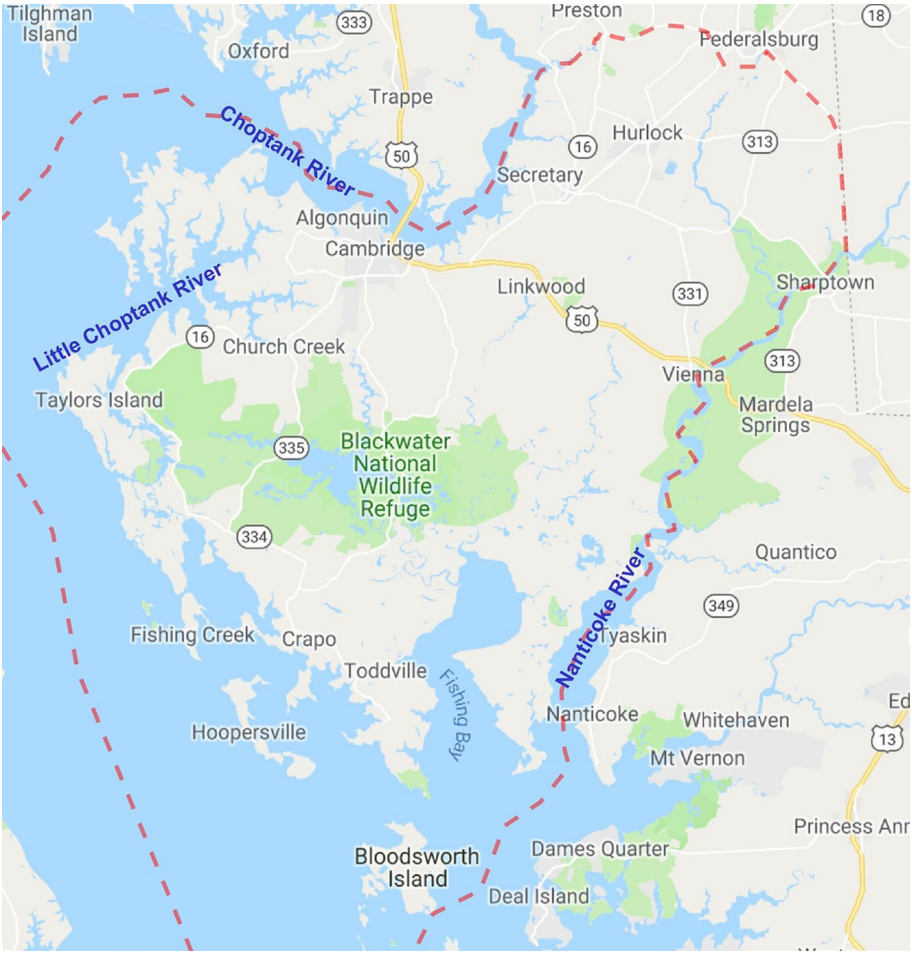

Fig. 6 Geographic map of Dorchester County, Maryland

the banks of Choptank River and Nanticoke River (see Fig. 6 for their locations). More noticeably, water depth in the inundated areas is substantially higher, reaching 2.5–3 m in deepest places. Moreover, the projected inundated areas and inundation depths are quite different in 2100 between RCP 4.5 and 8.5.

In 2100, there are substantial differences in the overland inundation among the GCMs in each climate change scenario, reflecting larger uncertainty in climate projections at the end of twenty-first century (Fig. 8). The inundation depths display large differences among the lower range, median and upper range of RCP 4.5 projections (Fig. 8 a–c). The inundation depths under RCP 8.5 are considerably larger than those under RCP 4.5, but show smaller differences among the lower, median and upper projections (Fig. 8 a–f).

Figure 9 summarizes the total inundated area and average inundation depth for different climate change scenarios. Hurricane Isabel was estimated to flood 825 km^2 in Dorchester County (Fig. 9a). By 2050, the total inundated area in Dorchester County rises to ~ 885 km^2 under the median projections of both RCP 4.5 and 8.5, with a range of 875 km^2 to

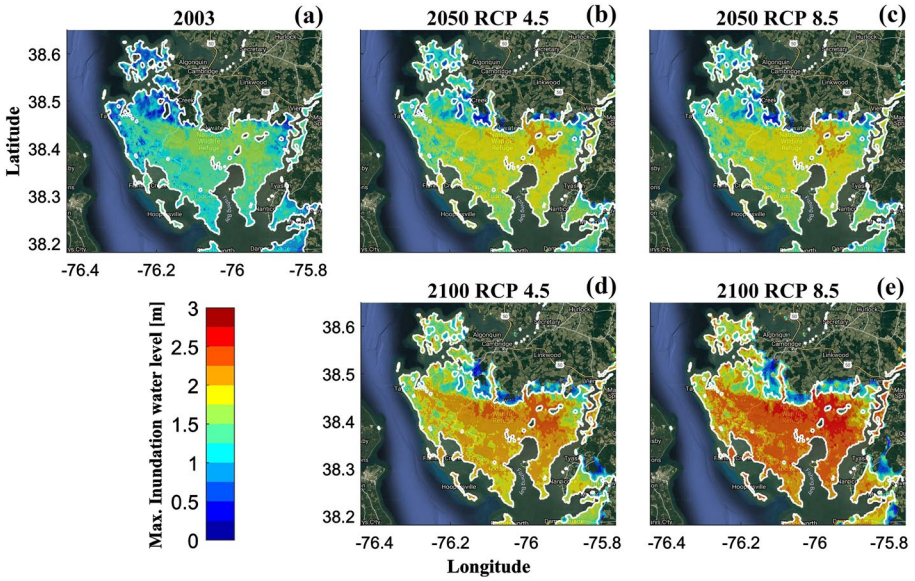

Fig. 7 Model predicted inundated area in Dorchester County, MD, during Hurricane Isabel (**a**) and Isabel-like storms in 2050 (**b**, **c**) and 2100 (**d**, **e**) under the median projections of RCP 4.5 (**b**, **d**) and RCP 8.5 (**c**, **e**)

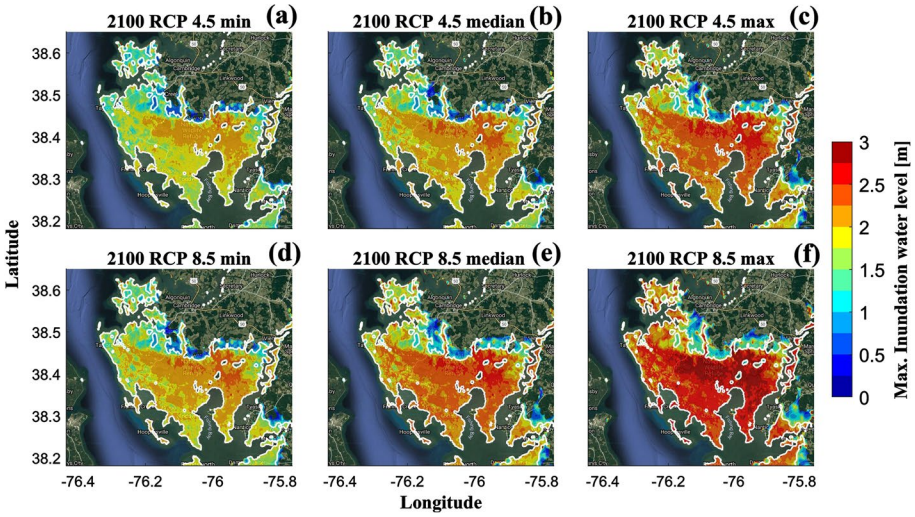

Fig. 8 Model predicted inundated area in Dorchester County, MD, during Isabel-like storms in 2100 under the lower (left), median (middle), and upper (right) projections of RCP 4.5 (top) and RCP 8.5 (bottom)

903 km^2 between the lower and upper range of the climate model projections. By 2100, the total inundated area increases to 919 km^2 under the median projection of RCP 4.5 and 942 km^2 under the median projection of RCP 8.5. The range of the projected inundated area in Dorchester is smaller under RCP 4.5 (42 km^2) than under RCP 8.5 (55 km^2). Flood damage typically increases disproportionately with flood depth (Scawthorn et al. 2006a, b).

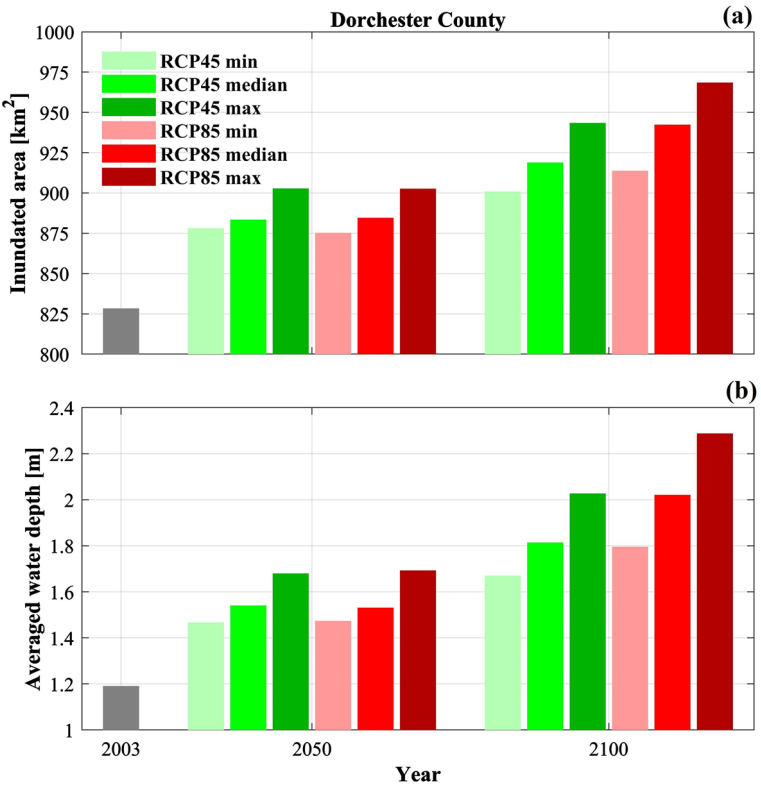

Fig. 9 The total inundated area and the average water depth over the inundated land in Dorchester County, MD, for Hurricane Isabel (2003) and Isabel-like storm in 2050 and 2100 under RCP 4.5 and 8.5

The average inundation depth in Dorchester County was just under 1.2 m during Hurricane Isabel, but increases to ~ 1.55 m under the median projections of RCP 4.5 and 8.5 in 2050 (Fig. 9b). In 2100, the inundation depth increases to 1.81 m under the median projection of RCP 4.5 and 2.02 m under the mean projection of RCP 8.5, representing 51–68% increase in the inundation depth. Once again, the spread in the inundation depth is smaller under RCP 4.5 (0.36 m) than under RCP 8.5 (0.49 m).

The model-predicted inundated areas were overlaid over the map of existing homes in Dorchester County to estimate the total number of houses flooded during Hurricane Isabel and Isabel-like storms in the future climate (Fig. 10a). Isabel flooded about 1420 houses. Although the storm in 2050 floods more land areas, it floods 80 less houses under the median projection of RCP 4.5 because most of the additional flooded areas are not on residential areas and some of the areas flooded by Isabel are not flooded by the storm in the future. However, the storm is projected to flood about 1,740 houses under the high end projection of RCP 4.5. Although the flooded area under the median projection of RCP 8.5 is only marginally larger than that under the median projection of RCP 4.5, 420 more houses are flooded because the additional flooding hit residential areas. By 2100, 1,850 houses are predicted to be flooded in Dorchester County under the median projection of RCP 4.5 but over 2,190 houses are flooded under the median projection of RCP 8.5. There are large differences in the number of flooded houses (~ 400 to 500 houses) between the high and

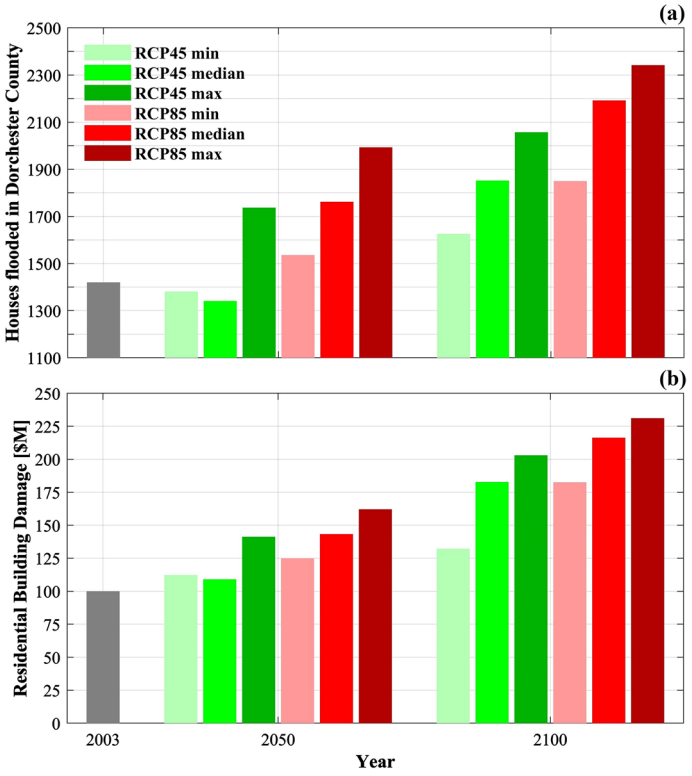

Fig. 10 **a** Number of houses affected by flooding and **b** estimated property damage in Dorchester County due to Hurricane Isabel (2003) and Isabel-like storm in 2050 and 2100 under RCP 4.5 (green) and RCP 8.5 (red) scenarios

low ends of climate model projections under both RCP 4.5 and RCP 8.5, suggesting larger uncertainty in predicting flooded houses in 2100.

With an average home size of 1500 ft^2 in Dorchester County, we can estimate flood damage to residential buildings by using the depth-damage function (Scawthorn et al. 2006a, b; HAZMAT 2014), as shown in Fig. 10b. Because the model does not have the spatial resolution to resolve each house and lot, we used the mean inundation depth in the flooded areas to obtain an estimate for the property damage. The damage to residential houses was estimated to be ~ $100 million during Hurricane Isabel and would increase to $109/143 million in 2050 and $183/216 million in 2100 under RCP4.5/8.5. Combing the housing data with the census data, we estimated that the flooding due to Hurricane Isabel directly affected about 3,351 people. Under the median climate change projections, a similar storm affects 3,162/4,106 people (RCP 4.5/RCP 8.5) in 2050 and 4,366/5,168 people (RCP 4.5/RCP 8.5) in 2100.

3.3 City of Baltimore

Downtown Baltimore is situated next to the Inner Harbor which is connected to Patapsco River, a tributary of Chesapeake Bay (Fig. 11). Hundreds of businesses are found in the

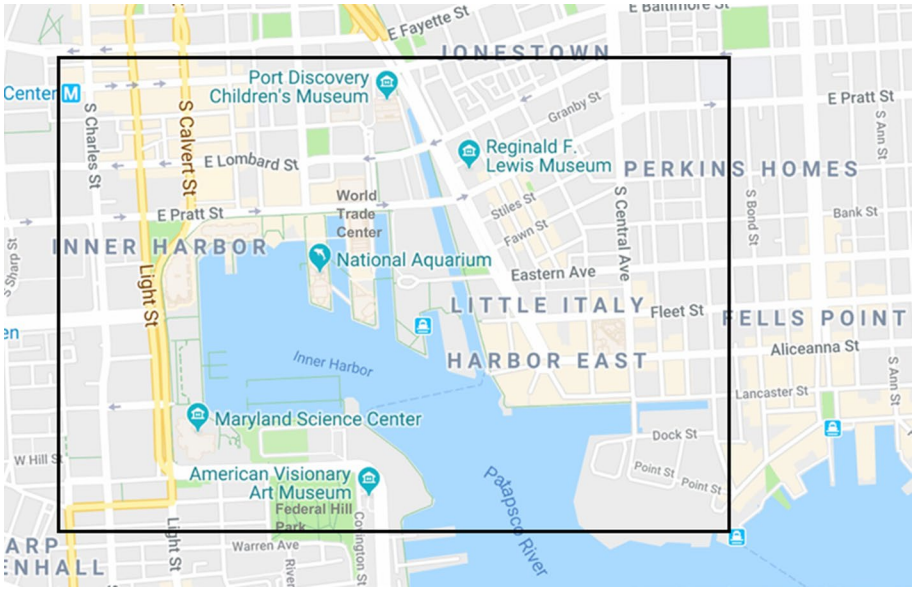

Fig. 11 Map of downtown Baltimore, Maryland. The thick black box marked the area shown in Fig. 12

downtown financial district, including skyscrapers like the Bank of America building and the Baltimore World Trade Center. Both Charles Street and Pratt Street are significant avenues of commercial and cultural activity. The Inner Harbor itself is the chief commercial and tourist destination in Baltimore, visited by over 13 million people a year. It is home to museums such as the Maryland Science Center, the National Aquarium in Baltimore and the Flag House & Star-Spangled Banner Museum. To the west of the Inner Harbor are the Light street and Charles Street where land elevation rises rather rapidly. South of the Inner Harbor lies museums, Federal Hill Park and apartment buildings. North of the Inner Harbor lies in Pratt Street and business buildings. To the northeast of the Inner Harbor lies in Fells Point and Little Italy featuring residential buildings and restaurants, with many low-lying areas.

When Hurricane Isabel hit in 2003, it flooded streets around the Inner Harbor (Fig. 12a), with Pratt Street and Light Street as well as streets in Fells Point and Little Italy under water. The predicted inundated area is in agreement with anecdotal reports of flooding in Baltimore (e.g., Fig. 1a). In 2050, the flooded area expands west of Light Street and north of Pratt Street and covers a large area in Little Italy and Fells Point, according to the median projection of RCP 8.5 (Fig. 12b). In 2100, the flooding reaches Charles Street in the west and 2 blocks north of Pratt Street (Fig. 12c). Several blocks in Little Italy and Fells Point are also flooded. The total inundated area in Baltimore was 2.2 km^2 during Hurricane Isabel, increases to 5.1 km^2 in 2050 under the median projections of RCP 4.5 and 8.5, and expands ~ 4 times to 8.1/9.1 km^2 under RCP 4.5/8.5 in 2100 (Fig. 13a). Interestingly, the average inundation depth was about 1.13 m during Isabel but reduces slightly to 1–1.12 m under all climate change scenarios in 2050 (Fig. 13b). The flooded areas during Hurricane Isabel were low-lying land right at the water front. As more areas are flooded in 2050, the land elevation rises such that the averaged inundation depth is smaller even though the peak water level is higher. In 2100, as more land areas are flooded, the inundation depth

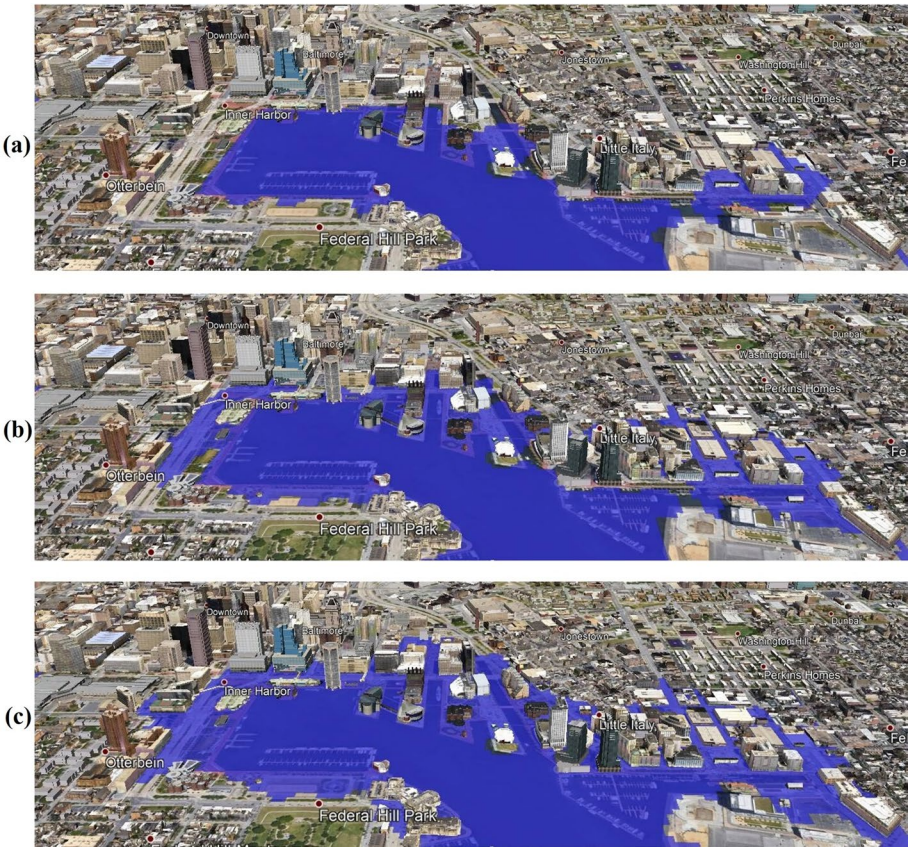

Fig. 12 Model predicted inundated area in Baltimore, MD during Hurricane Isabel (**a**) and Isabel-like storms in 2050 (**b**) and 2100 (**c**) under the median projection of RCP 8.5

increases to 1.17/1.28 m under the median projection of RCP 4.5/8.5. The inundation depth also expands a wider range in 2100 under RCP 8.5, with the largest inundation depth at 1.51 m and the smallest inundation depth at 1.15 m.

How do these inundated areas translate to potential economic loss to the City of Baltimore? First the Google map was used to calculate the percentage (the total square footage) of the flooded areas that are occupied by buildings. Then the total depth-damage function for commercial buildings, expressed in terms of a unit cost per m^2 (Huizinga et al. 2017), was used to estimate the flood cost to these buildings. Again we use the total damage function that includes the structure and content costs. We estimated a loss of $29 million in downtown Baltimore during Hurricane Isabel (Fig. 14). It is further assumed that the property values are indexed in today's dollars, given the difficulty in forecasting future price movements in real estate. In 2050, the estimated economic cost due to an Isabel-like storm is estimated to be $98 million under RCP 4.5 but $100/$115 million under the median/high end projections of RCP 8.5 (Fig. 14). This represents three–fourfold increases in the economic damage to downtown Baltimore. There are relatively small differences in the estimated damage ($94–$115 million) among different climate change scenarios and different climate models. By 2100, the economic loss increases to $150/$162 million under the

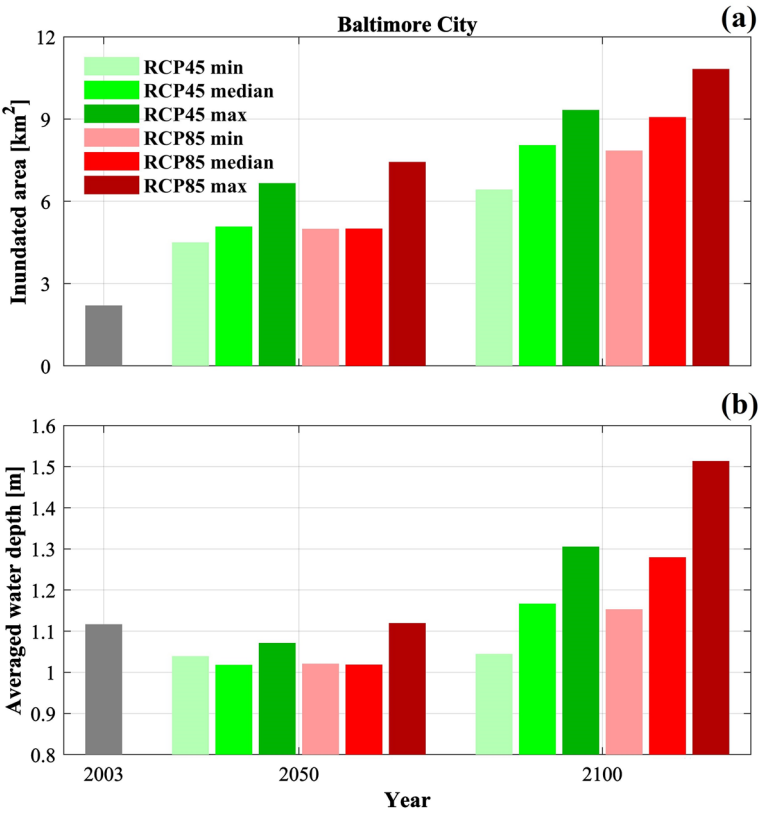

Fig. 13 The total inundated area (**a**) and the average water depth (**b**) over the inundated land in the City of Baltimore, MD for Hurricane Isabel (2003) and Isabel-like storm in 2050 and 2100 under RCP 4.5 and 8.5

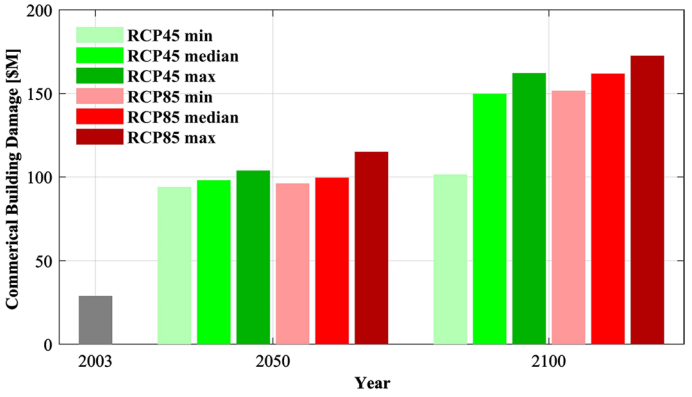

Fig. 14 Estimated flood damage to commercial buildings in the City of Baltimore based on the depth-damage function

median projections of RCP 4.5/8.5 (Fig. 14). The highest end projection of RCP 8.5 results in a total economic loss of $173 million to the City of Baltimore. This represents nearly 6 times increase in the property damage, with huge economic consequences. The estimated flood damage in 2100 varies from $102 to $162 million, depending on whether the low or upper projection of RCP 4.5 is used in the calculations. It ranges from $152 to $173 million under RCP 8.5.

4 Discussion and conclusion

Using the climate model projections to drive regional atmosphere–ocean models, we have investigated how ocean warming and sea level rise affect storm surge and coastal inundation in Chesapeake Bay. Warming ocean produces more intense storms and stronger winds, resulting in higher storm surge and more extensive flooding. Hurricane Isabel (2003) generated a peak water level of 1.6 m in Cambridge and 2.2 m in Baltimore, Maryland. By 2100, the peak water level is projected to reach 2.5/2.7 m in Cambridge and 3.2/3.4 m in Baltimore under RCP 4.5/8.5. The net increase of 0.9/1.1 m in Cambridge is slightly larger than the projected sea level rise of 0.85/1.06 m. However, in the upper-estuary location Baltimore, the peak water level increases by 1.0/1.2 m under RCP 4.5/8.5, representing 18%/13% over the sea level rise. In terms of overland inundation, Isabel flooded 1850 km^2. By 2100, an Isabel-like storm floods 2715 km^2 under RCP 4.5 median scenario and 3000 km^2 under RCP 8.5 median scenario. Sea level rise alone flooded 1184/1484 km^2 under RCP 4.5/8.5, and the storm surge flooded additional 1531/1586 km^2. Our modeling study has illustrated the nonlinear effects of sea level rise, storm surge and land topography on coastal inundation.

The rural and urban areas show quite different responses to climate change, due to differences in land topography and geography. Over the rural Dorchester County, the inundated area shows moderate expansion in the future climate, but the average inundation depth is ~ 30% higher in 2050 and ~ 50 to 70% higher in 2100. The number of houses flooded increases from 1420 during Hurricane Isabel to 1850/2190 in 2100 under the climate change scenario RCP 4.5/8.5. The estimated total flood damage in Dorchester County increases from $100 million in 2003 to $183/$216 million in 2100 under the median projection of RCP 4.5/8.5. In comparison, the inundated area in the City of Baltimore is projected to expand fourfold: The flooded area was estimated to be 2.2 km^2 during Hurricane Isabel and is projected to expand to 5.1 km^2 in 2050 and 8.1/9.1 km^2 in 2100 under RCP 4.5/8.5. Given the intense economic activities in the water front areas in Downtown Baltimore, these large expansions of the inundated areas would translate to large increases in economic damages. The estimated property loss increases from $29 million in 2003 to $100 million in 2050 and $150/$162 million in 2100 under RCP 4.5/8.5. There are uncertainties in projecting future coastal inundation impacts and economic damage due to uncertainties in climate change scenarios and inter-model differences among climate models. In 2100, the estimated property damage ranges from $132 million to $231 million in Dorchester County. It ranges from $102 million to $173 million in downtown Baltimore.

One limitation of this study is the assumption of uniform relative sea level rise. The rates of land subsidence in Chesapeake Bay are spatially variable. For example, by 2100 the relative sea level rise in Norfolk is projected be 10 cm larger than that in Baltimore and Washington, D.C., which is about 10% of the sea level rise (Boesch et al. 2018). Ralston et al. (2019) reconstructed bathymetry changes in the Hudson River between 1860 s and

2016 using historical charts. A similar approach could be used to consider the effects of variable land subsidence in Chesapeake Bay. Instead of the historical charts, we would need projections of vertical land motion for the twenty-first century.

In this study, we focused on Category 2 Hurricane Isabel (2003) and its cousins in the future climate because Isabel was considered as a 100-year flooding event for planning purposes by cities and towns around Chesapeake Bay. To obtain a comprehensive assessment of flood risks, however, we would need to model storms of various return periods (say 10–100 years). The probabilistic approach to sea level rise projections (Kopp et al. 2014, 2017) would naturally fit into this risk assessment. To generate an ensemble of storms appropriate for probabilistic calculations, one would need to analyze the past storm climatology and consider how climate change might affect the storm climatology. It is computationally expensive to conduct these model runs. Many previous studies represented storms with the parametric wind model using parameters such as the central pressure deficit, the storm size, the forward propagation speed, the storm heading and the landfall location, and employed joint probability method (JPM)-optimal sampling (OS) schemes to select representative storms (Toro et al. 2010a, b; Niedoroda et al. 2010; Condon and Sheng 2012). Others used a statistical deterministic hurricane model (Emanuel et al. 2006) to generate synthetic storms under the large-scale atmospheric and oceanic environments projected by GCMs (Lin et al. 2012, 2016). These hurricane models are computationally efficient, but they cannot capture mesoscale wind structures and wind speed asymmetry in hurricanes and produce accurate wind predictions needed for accurate storm surge predictions. Short-term storm-surge forecasts now use mesoscale atmospheric models to forecast winds, and our study is one of the few that use such a model to obtain realistic simulations of hurricanes under changing climate conditions. The feasibility of our approach has been demonstrated. With increasing computational power, it could be used to obtain a probabilistic risk assessment of coastal inundation in the future climate. The inundation maps obtained from this modeling approach would be more realistic than the traditional floodplain maps generated from the parametric wind model.

Many fringe areas of Chesapeake Bay are covered by salt marshes which are not simulated in our model. Coastal wetlands may defend coastal communities from storm surge and sea level rise and mitigate coastline erosion (Reza et al. 2016; Kirwan et al. 2016; Rezaie et al. 2020). During storm floods, drag in vegetation on wetlands decelerates water flows and reduces marsh erosion. It would be interesting to consider these dynamic interactions between storm-induced flows and vegetation in a future study. An intermediate step might be to prescribe a drag coefficient using empirically determined Manning's coefficient to represent different types of vegetative surfaces such as coastal wetlands, forests, and farms (Bunya et al. 2010; Dietrich et al. 2011; Ferreira et al. 2014). As sea level rises, coastal morphology continually adapts toward equilibrium and salt marsh might migrate upstream. An integrated modeling system, consisting of submodels of hydrodynamics, surface waves, sediment transport (e.g., Warner et al. 2010; Xie et al. 2018), ecogeomorphology (Lesser et al. 2004; Nardin and Edmonds 2014), and engineered shoreline structures (Ge et al. 2012), would need to be developed in order to simulate the evolving coastlines and coastal inundation under changing climate.

When assessing potential economic damages due to coastal flooding, we used simple depth-damage functions. This depth-damage approach does not include potential wave damage, although waves are relatively weak in semi-enclosed bays and estuaries such as Chesapeake Bay. Future work could consider cost–benefit analysis of various mitigation and adaptation measures in reducing inundation impacts, following similar approaches as Neumann et al. (2015) and Diaz (2016) among others. Zhang and Li (2019) compared the

storm surge height in Chesapeake Bay between two model runs: one soft shoreline scenario which allows low-lying areas to be flooded; one hard shoreline scenario which prevents flooding at the current coastline. They found that hardening shorelines would increase the surge height in the upper parts of the estuary by 0.5 m. A future extension of this work could examine different shoreline scenarios such as adaptation measures in low-lying rural areas and installation of engineered structures around urban infrastructure. The costs of flood damage could then be compared against the costs of the mitigation and adaptation measures to identify most cost-effective ways to bolster coastal resiliency in the entire region.

Acknowledgements We are grateful to two reviewers for the helpful comments. Funding support was provided by Maryland Sea Grant (NA14OAR4170090 and SA75281450-H). Fan Zhang is supported by Maryland Sea Grant Fellowship. This is UMCES contribution number 5868.

Data Availability The inundation graphics are hosted at https://geronimo.hpl.umces.edu/mingli/. Model output is available at https://doi.org/10.5281/zenodo.3497531.

References:s

Amante C, Eakins BW (2009) ETOPO1 Global Relief Model converted to PanMap layer format, NOAA-Natl. Geophys. Data Cent., Boulder. https://doi.org/10.1594/pangaea.769615

Bengtsson L, Botzet M, Esch M (1996) Will greenhouse-induced warming over the next 50 years lead to higher frequency and greater intensity of hurricanes? Tellus 48A:57–73

Bilskie MV, Hagen SC, Alizad KA, Medeiros SC, Passeri DL, Needham H (2016) Dynamic simulation and numerical analysis of hurricane storm surge under sea level rise with geomorphologic changes along the northern Gulf of Mexico. Earth's Future 4(5):177–193

Boesch DF et al (2018) Sea-level Rise: Projections for Maryland 2018, 27 pp. University of Maryland Center for Environmental Science, Cambridge

Bunya S, Dietrich JC, Westerink JJ et al (2010) A high resolution coupled riverine flow, tide, wind, wind wave and storm surge model for southern Louisiana and Mississippi: Part I—model development and validation. Mon Wea Rev 138:345–377

Chen C, Liu H, Beardsley RC (2003) An unstructured grid, finite-volume, three-dimensional, primitive equations ocean model: application to coastal ocean and estuaries. J Atmos Ocean Tech 20:159–186

Chen C, Beardsley RC, Cowles G (2006) An unstructured grid, finite-volume coastal ocean model (FVCOM) system. Oceanography 19(1):78–89

Chen C et al (2011) An unstructured-grid, finite-volume community ocean model fvcom user manual, 3rd edn. SMAST/UMASSD-11-1101

Chen C et al (2013) Extratropical storm inundation testbed: Intermodel comparisons in Scituate. Massachusetts. J Geophys Res Ocean 118:5054–5073. https://doi.org/10.1002/jgrc.20397

Condon AJ, Sheng PY (2012) Evaluation of coastal inundation hazard for present and future climates. Nat Hazards 62:345–373

Church JA et al (2013) Sea level change. In: Stocker TF, et al. (eds) Climate change 2013: the physical science basis. Contribution of working Group I to the fifth assessment report of the intergovernmental panel on climate change, Cambridge Univ, Press, pp 1137–1216

Church JA, White NJ (2011) Sea-level rise from the late 19th to the early 21st century. Surv Geophys 32:585–602

Dangendorf S, Marcos M, Wöppelmann G, Conrad CP, Frederikse T, Riva R (2017) Reassessment of 20th century global mean sea level rise. PNAS. https://doi.org/10.1073/pnas.1616007114

Davis C et al (2008) Prediction of landfalling hurricanes with the Advanced Hurricane WRF model. Mon Wea Rev 136:1990–2005

DeConto RM, Pollard D (2016) Contribution of Antarctica to past and future sea-level rise. Nature 531:591–597

Diaz DB (2016) Estimating global damages from sea level rise with the Coastal Impact and Adaptation Model (CIAM). Clim Change 137(1–2):143–156

Dietrich JC, Zijlema M, Westerink JJ et al (2011) Modeling hurricane waves and storm surge using integrally-coupled, scalable computations. Coast Eng 58:45–65. https://doi.org/10.1016/j.coastaleng.2010.08.001
Dinan T (2017) Projected increases in hurricane damage in the United States: The role of climate change and coastal development. Ecol Econ 138:186–198
Ding A, White JF, Ullman PW, Fashokun AO (2008) Evaluation of HAZUS-MH flood model with local data and other program. Nat Hazards Rev 9(1):20–28
Domingues CM, Church JA, White NJ, Gleckler PJ, Wijffels SE, Barker PM, Dunn JR (2008) Improved estimates of upper-ocean warming and multi-decadal sea-level rise. Nature 453:1090–1093
Domingues R, Goni G, Baringer M, Volkov D (2018) What caused the accelerated sea level changes along the United States East Coast during 2010–2015? Geophys Res Lett. https://doi.org/10.1029/2018GL081183
Egbert GD, Erofeeva SY (2002) Efficient inverse modeling of barotropic ocean tides. J Atmos Ocean Tech 19(2):183–204
Eichler TP, Gaggini N, Pan Z (2013) Impacts of global warming on Northern Hemisphere winter storm tracks in the CMIP5 model suite. J Geophys Res Atmos 118(10):3919–3932
El-Sabh MI (1990) Statistical analysis of long-term storm surge data, storm surge: observation and modeling. In: Proceedings of international symposium on storm surge. China Ocean Press, Beijing, pp 313–314
Emanuel KA (2006) Climate and tropical cyclone activity: a new model downscaling approach. J Clim 19:4797–4802
Emanuel KA, Ravela S, Vivant E, Risi C (2006) A statistical deterministic approach to hurricane risk assessment. Bull Am Meteor Soc 87:299–314
Emanuel KA (2008) The Hurricane-climate connection. Bull Am Meteor Soc 89:ES10–ES20
Emanuel KA (2013) Downscaling CMIP5 climate models shows increased tropical cyclone activity over the 21st century. In: Proceedings of the National Academy of Science. www.pnas.org/cgi/doi/10.1073/pnas.1301293110
Engelhart SE, Horton BP, Douglas BC, Peltier WR, Törnqvist TE (2009) Spatial variability of late Holocene and 20th century sea level-rise along the Atlantic coast of the United State. Geology 37:1115–1118
Ezer T (2013) Sea level rise, spatially uneven and temporally unsteady: why the U.S. East Coast, the global tide gauge record and the global altimeter data show different trends. Geophys Res Lett 40(20):5439–5444
Ezer T, Atkinson LP, Corlett WB, Blanco JL (2013) Gulf Stream's induced sea level rise and variability along the U.S. mid-Atlantic coast. J Geophys Res Oceans 118:685–697
Ezer T, Corlett WB (2012) Is sea level accelerating in the Chesapeake Bay? A demonstration of a novel new approach for analyzing sea level data. Geophys Res Lett 39:L19065. https://doi.org/10.1029/2012GL053435
Familkhalili R, Talke SA (2016) The effect of channel deepening on tides and storm surge: a case study of Wilmington, NC. Geophys Res Lett 43:9138–9147. https://doi.org/10.1002/2016GL069494
Ferreira CM, Irish JL, Olivera F (2014) Uncertainty in hurricnae surge simulation due to land cover specification. J Geophys Res Oceans 119:1812–1827. https://doi.org/10.1002/2013JC009604
Ge J, Chen C, Qi J, Ding P, Beardsley (2012) A dike-groyne algorithm in a terrain-following ocean model (FVCOM): development, validation and application. Ocean Model 47:26–41
Gesch DB (2009) Analysis of Lidar elevation data for improved identification and delineation of lands vulnerable to sea level rise. J Coast Res 53:49–58
Grothe P, Taylor LA, Eakins BW, Warnken RR, Carignan KS, Lim E, Caldwell RJ, Friday DZ (2010) Digital elevation model of Ocean City, Maryland: procedures, data sources, and analysis. NOAA Tech. Memo. NESDIS NGDC-37, Dept. of Commerce, Boulder
Hagen SC, Bacopoulos P (2012) Synthetic storms contributing to coastal flooding in Florida's Big Bend Region with application to sea level rise. Terr Atmos Ocean Sci 23(5):481–500
Hallegatte S, Green C, Nicholls RJ, Corfee-Morlot J (2013) Future flood losses in major coastal cities. Nat Clim Change 3(9):802–806
Hauer ME, Evans JM, Mishra DR (2016) Millions projected to be at risk from sea-level rise in the continental Unites States. Nat Clim Change. https://doi.org/10.1038/NCLIMATE2961
Hay CC, Morrow E, Kopp RE, Mitrovica JX (2015) Probabilistic reanalysis of twentieth-century sea-level rise. Nature 517:481–484
HAZUS (2014) The Federal Emergency Management Agency's (FEMA's) methodology for estimating potential losses from diasters. https://www.fema.gov/hazus/
Hill KA, Lackmann GM (2011) The impact of future climate change on TC intensity and structure: a downscaling approach. J Clim 24(17):4644–4661

Hinkel J, Dp V, Nicholls RJ, Klein RJT (2013) The effects of miigation and adaptation on coastal impacts in the 21st century. Clim Change 117:783394
Hinkel J et al (2014) Coastal flood damage and adaptation costs under 21st century sea-level rise. Proc Natl Acad Sci USA 111(9):3292–3297
Holleman RC, Stacey MT (2014) Coupling of sea level rise, tidal amplification, and inundation. J Phys Oceanogr 44(5):1439–1455
Horsburgh KJ, Wilson C (2007) Tide-surge interaction and its role in the distribution of surge residuals in the North Sea. J Geophy Res Oceans 112:C08003. https://doi.org/10.1029/2006JC004033
Huizinga J, Moel H, de Szewczyk W (2017) Global flood depth-damage functions. Methodology and the database with guidelines. EUR 28552 EN. https://doi.org/10.2760/16510.
IPCC (2013) Climate change 2013: the physical science basis. Working Group I Contribution to the IPCC 5th Assessment Report - Changes to the Underlying Scientific/Technical Assessment (IPCC-XXVI/Doc.4)
Kerr PC et al (2013) US IOOS coastal and ocean modeling testbed: Inter-model evaluation of tides, waves, and hurricane surge in the Gulf of Mexico. J Geophys Res Ocean 118:5129–5172. https://doi.org/10.1002/jgrc.20376
Kirwan ML, Walters DC, Reay WG, Carr JA (2016GL) Sea level driven marsh expansion in a coupled model of marsh erosion and migration. Geophys Res Lett 43:4366–4373. https://doi.org/10.1002/2016GL068507
Knutson TR et al (2013) Dynamical downscaling projections of twenty-first-century Atlantic hurricane activity: CMIP3 and CMIP5 model-based scenarios. J Clim 26(17):6591–6617
Knutson TR, Tuleya RE (2004) Impact of CO2-induced warming on simulated hurricane intensity and precipitation: Sensitivity to the choice of climate model and convective parameterization. J Clime 17:3477–3495
Kopp RE (2013) Does the mid-Atlantic United States sea level acceleration hot spot reflect ocean dynamic variability? Geophys Res Lett 40(15):3981–3985
Kopp RE et al (2014) Probabilistic 21st and 22nd century sea-level projections at a global network of tide gauge sites. Earth's Future 2:287–306
Kopp RE et al (2017) Implications of Antarctic ice-cliff collapse and ice-shelf hydrofracturing mechanisms for sea-level projections. Earth's Future 5:1217–1233
Kulp S, Strauss BH (2017) Rapid escalation of coastal flood exposure in US municipalities from sea level rise. Clim Change. https://doi.org/10.1007/s10584-017-1963-7
Lee SB, Li M, Zhang F (2017) Impact of sea level rise on tidal range in Chesapeake and Delaware Bays. J Geophys Res Oceans 122(5):3917–3938
Lesser G, Roelvink J, Van Kester J, Stelling G (2004) Development and validation of a three-dimensional morphological model. Coast Eng 51:883–915
Li M, Zhong L, Boicourt WC, Zhang S, Zhang DL (2006) Hurricane-induced storm surges, currents and destratification in a semi-enclosed bay. Geophys Res Lett 33:L02604. https://doi.org/10.1029/2005GL024992
Li M, Zhong L, Boicourt WC, Zhang S, Zhang DL (2007) Hurricane-induced destratification and restratification in a partially-mixed estuary. J Mar Res 65:169–192
Lin N, Emanuel K, Oppenheimer M, Vanmarcke E (2012) Physically based assessment of hurricane surge threat under climate change. Nat Clim Change 2(6):462
Lin N, Kopp RE, Horton BP, Donnelly JP (2016) Hurricane Sandy's flood frequency increasing from year 1800 to 2100. Proc Nat Acad Sci 113(43):12071–12075
Lowe JA, Gregory JM (2005) The effects of climate change on storm surges around the United Kingdom. Philos Trans R Soc Lond A 363(1831):1313–1328
Mallard MS, Lackmann GM, Aiyyer A, Hill K (2013a) Atlantic hurricanes and climate change. Part I: experimental design and isolation of thermodynamic effects. J Clim 26(13):4876–4893
Mallard MS, Lackmann GM, Aiyyer A (2013b) Atlantic hurricanes and climate change. Part II: role of thermodynamic changes in decreased hurricane frequency. J. Climate 26(21):8513–8528
McAlpine SA, Porter JR (2018) Estimating recent local impacts of sea-level rise on current real-estate losses: a housing market case study in Miami-Dade. Florida Popul Res Policy Rev 37:871–895
McNamara DE, Gopalakrishnan S, Smith MD, Murray AB (2015) Climate adaptation and policy-induced inflation of coastal property value. PLoS ONE 10:e0121278
Marcos M, Calafat FM, Berihuette A, Dangendorf S (2015) Long-term variations in global sea level extremes. J Geophys Res Oceans 120:8115–8134. https://doi.org/10.1002/2015JC011173
McInnes KL, Walsh KJE, Hubbert GD, Beer T (2003) Impact of sea-level rise and storm surges on a coastal community. Nat Hazards 30(2):187–207

Mikhailova MV (2011) Interaction of tides and storm surges at the Elbe River Mouth. Water Res 38(3):284–297
Miller KG, Kopp RE, Horton BP, Browning JV, Kemp AC (2013) A geological perspective on sea-level rise and its impacts along the US mid-Atlantic coast. Earth's Fut 1(1):3–18
Mitchell M, Hershner C, Herman J, Schatt D, Mason P, Eggington E (2012) Recurrent flooding study for tidewater Virginia. Report of the Virginia Institute of Marine Science to the Governor and the General Assembly of Virginia
Moftakhari HR, AghaKouchak A, Sanders BF, Feldman DL, Sweet W, Matthew RA, Luke A (2015) Increased nuisance flooding along the coasts of the United States due to sea level rise: past and future. Geophys Res Lett 42:9846–9852
Moss RH et al (2010) The next generation of scenarios for climate change research and assessment. Nature 463:747–756
Mousavi ME, Irish JL, Frey AE, Olivera F, Edge BL (2011) Global warming and hurricanes: the potential impact of hurricane intensification and sea level rise on coastal flooding. Clim Change 104(3–4):575–597
Nardin W, Edmonds DA (2014) Optimum vegetation height and density for inorganic sedimentation in deltaic marshes. Nat Geosci. https://doi.org/10.1038/ngeo2233
Neumann J, Hudgens D, Herter J, Martinich J (2011) The economics of adaptation along developed coastlines. Clim Change 2:89–98. https://doi.org/10.1002/wcc.90
Neumann J, Emanuel K, Ravela S, Ludwig L, Kirshen P, Bosma K, Martinich J (2015) Joint effects of storm surge and sea-level rise on US Coasts: new economic estimates of impacts, adaptation, and benefits of mitigation policy. Clim Change 129:337–349
Niedoroda AW, Resio DT, Toro GR, Divoky D, Das HS, Reed CW (2010) Analysis of the coastal Mississippi storm surge hazard. J Ocean Eng. https://doi.org/10.1016/j.oceaneng.2009.08.019
Nicholls RJ (2004) Coastal flooding and wetland loss in the 21st century:changes under the SRES climate and socio-economic scenarios. Glob Environ Change 14(1):69–86
Nolan DS, Zhang JA, Stern DP (2009a) Evaluation of planetary boundary layer parameterizations in tropical cyclones by comparison of in situ observations and high-resolution simulations of Hurricane Isabel (2003). Part I: Initialization, maximum winds, and the outer-core boundary layer. Mon Wea Rev 137:3651–3674
Nolan DS, Zhang JA, Stern DP (2009b) Evaluation of planetary boundary layer parameterizations in tropical cyclones by comparison of in situ observations and high-resolution simulations of Hurricane Isabel (2003). Part II: Inner-Core Boundary Layer and Eyewall Structure. Mon Wea Rev 137:3675–3698
Orton P et al (2015) New York city panel on climate change 2015 report: Dynamic coastal flood modeling. Ann N Y Acad Sci 1336(1):56–66
Orton P, Conticello F, Cioffi F, Hall T, Georgas N, Lall U, Blumberg A, MacManus K (2018) Hazard assessment from storm tides, rainfall and sea level rise on a tidal river estuary. Nat Hazards 1–29
Palinkas CM, Sanford LP, Koch EW (2017) Influence of shoreline stabilization structures on the nearshore sedimentary environment in mesohaline Chesapeake Bay. Estuaries Coasts. https://doi.org/10.1007/s12237-017-0339-6
Patrick CJ, Weller DE, Li X, Ryder M (2014) Effects of shoreline alteration and other stressors on submerged aquatic vegetation in subestuaries of Chesapeake Bay and the Mid-Atlantic coastal bays. Estuaries Coasts 37:1516–1531. https://doi.org/10.1007/s12237-014-9768-7
Peng M, Xie L, Pietrafesa LJ (2004) A numerical study of storm surge and inundation in the Croatan–Albemarle–Pamlico estuary system. Est Coast Shelf Sci 59:121–137. https://doi.org/10.1016/j.ecss.2003.07.010
Piecuch CG, Bittermann K, Kemp AC, Ponte RM, Little CM, Engelhart SE, Lentz SJ (2018) River-discharge effects on United States Atlantic and Gulf coast sea-level changes. PNAS 115(30):7729–7734. https://doi.org/10.1073/pnas.1805428115
Ralston DK, Talke SA, Geyer WR, Al-Zubaidi HAM, Sommerfield CK (2019) Bigger tides, less flooding: effects of dredging on Barotropic dynamics in a highly modified estuary. J Geophys Res Oceans. https://doi.org/10.1029/2018JC014313
Reza M, Orton PM, Georgas N, Blumberg AF (2016) Three-dimensional hydrodynamic modeling of storm tide mitigation by coastal wetlands. Coast Eng 111:83–94
Rezaie AM, Loerzel J, Ferreira CM (2020) Valuing natural habitats for enhancing coastal resilience: wetlands reduce property damage from storm surge and sea level rise. PLoS ONE 15(1):e0226275. https://doi.org/10.1371/journal.pone.0226275
Sallenger A, Doran KS, Howard PA (2012) Hotspot of accelerated sea-level rise on the Atlantic coast of North America. Nat Clim Change 2:884–888

Scawthorn C et al (2006a) HAZUS-MH flood loss estimation methodology. I: Overview and flood hazard characterization. Nat Hazards Rev. 7(2):60–71
Scawthorn C et al (2006b) HAZUS-MH Flood loss estimation methodology. II: Damage and loss assessment. Nat Hazards Rev 7(2):72–81
Scheffner NW, Fitzpatrick PJ (1997) Real-time predictions of surge propagation. In: Spaulding ML, Blumberg AF (eds) Estuarine and coastal modeling. Amer. Soc. of Civ. Eng., pp 374–388
Seroka G, Miles T, Xu Y, Kohut J, Schofield O, Glenn S (2016) Hurricane Irene sensitivity to stratified coastal ocean cooling. Mon Wea Rev 144:3507–3530
Shen J, Wang HV, Sisson M, Gong W (2006) Storm tide simulation in the Chesapeake Bay using an unstructured grid model. Est Coast Shelf Sci 68(1–2):1–16
Skamarock WC, Klemp J, Dudhia J, Gill DO, Barker D, Duda MG, Powers JG (2008) A Description of the Advanced Research WRF Version 3. NCAR Technical Note NCAR/TN-475+STR
Smith DI (1994) Flood damage estimation—A review of urban stage-damage curves and loss functions. Water SA vol 20 No. 3 July 1994. ISSN 0378-4738
Smith JM, Cialone MA, Wamsley TV, McAlpin TO (2010) Potential impact of sea level rise on coastal surges in southeast Louisiana. Ocean Eng 37(1):37–47
Spanger-Siegfried E, Fitzpatrick MF, Dahl K (2014) Encroaching tides: How sea level rise and tidal flooding threaten U.S. East and Gulf Coast communities over the next 30 years. Union of Concerned Scientists, Cambridge
Sweet W, Park J (2014) From the extreme to the mean: Acceleration and tipping points of coastal inundation from sea level rise. Earth's Fut 2:579–600
Talke SA, Orton P, Jay DA (2014) Increasing storm tides in New York Harbor, 1944–2013. Geophys Res Lett 41:3149–3155. https://doi.org/10.1002/2014GL059574
Toro G, Niedoroda AW, Divoky D, Reed CW (2010a) Quadrature-based approach for the efficient calculation of surge hazard. J Ocean Eng. https://doi.org/10.1016/j.oceaneng.2009.09.005
Toro G, Resio DT, Divoky D, Niedoroda AW, Reed CW (2010b) Efficient joint probability methods for hurricane surge frequency analysis. J Ocean Eng. https://doi.org/10.1016/j.oceaneng.2009.09.004
USGCRP (2017) Climate Science Special Report: Fourth National Climate Assessment, volume I, edited by Wuebbles DJ et al. U.S. Global Change Research Program, Washington
Vecchi GA, Soden BJ (2007) Global warming and the weakening of the tropical circulation. J Clim 20(17):4316–4340
Villarini G, Vecchi GA (2012) Twenty-first-century projections of North Atlantic tropical storms from CMIP5 models. Nat Clim Change 2(8):604–607
Vuuren V et al (2011) The representative concentration pathways: an overview. Clim Change 109:5–31
Warner JC, Armstrong B, He R, Zambon JB (2010) Development of a coupled ocean–atmosphere–wave–sediment transport (COAWST) modeling system. Ocean Modeling 35(3):230–244
Woolings T, Gregory JM, Pinto JG, Reyers M, Brayshaw DJ (2012) Response of the North Atlantic storm track to climate change shaped by ocean-atmosphere coupling. Nat Goesci 5:313–317
Woth K, Weisse R, von Storch H (2006) Climate change and North Sea storm surge extremes: an ensemble study of storm surge extremes expected in a changed climate projected by four different regional climate models. Ocean Dyn 56(1):3–15
Wu S-Y, Najjar R, Siewert J (2009) Potential impacts of sea-level rise on the Mid- and Upper-Atlantic region of the United States. Clim Change 95:121–138
Xie X, Li M, Ni W (2018) Roles of wind-driven currents and surface waves in sediment resuspension and transport during a tropical storm. J Geophys Res. https://doi.org/10.1029/2018JC014104
Yang Z, Myers EP, Wong AM, White SA (2008) VDatum for Chesapeake Bay, Delaware Bay and adjacent coastal water areas: Tidal datums and sea surface topography, NOAA Technical Report NOS CS 15, 110 pp., NOAA, Silver Spring
Yang Z et al (2014) A modeling study of coastal inundation induced by storm surge, sea-level rise, and subsidence in the Gulf of Mexico. Nat Hazards 71(3):1771–1794
Yin J, Goddard PB (2013) Oceanic control of sea level rise patterns along the East Coast of the United States. Geophys Res Lett 40(20):5514–5520
Yin J, Griffies SM, Stouffer RJ (2010) Spatial variability of sea level rise in twenty-first century projections. J Clim 23(17):4585–4607
Yin J, Schlesinger ME, Stouffer RJ (2009) Model projections of rapid sea-level rise on the northeast coast of the United States. Nat Geosci 2(4):262
Zervas C (2001) Sea level variations of the United States, 1854-1999, NOAA Technical Report NOS CO-OPS 36
Zervas C (2009) Sea level variations of the United States 1854–2006. NOAA Technical Report NOS CO-OPS, 53

Zhang F, Li M, Ross AC, Lee SB, Zhang DL (2017) Sensitivity Analysis of Hurricane Arthur (2014) Storm surge forecasts to WRF physics parameterizations and model configurations. Wea Forecast 32(5):1745–1764

Zhang F, Li M (2019) Impacts of ocean warming, sea level rise and coastline management on storm surge in a semi-enclosed Bay. J Geophys Res. https://doi.org/10.1029/2019JC015445

Zhong L, Li M, Zhang DL (2010) How do uncertainties in hurricane model forecasts affect storm surge predictions in a semi-enclosed bay? Est Coast Shelf Sci 90(2):61–72